

VPE: Variational Policy Embedding for Transfer Reinforcement Learning

Isac Arnekvist, Danica Kragic and Johannes A. Stork¹

Abstract—Reinforcement Learning methods are capable of solving complex problems, but resulting policies might perform poorly in environments that are even slightly different. In robotics especially, training and deployment conditions often vary and data collection is expensive, making retraining undesirable. Simulation training allows for feasible training times, but on the other hand suffers from a reality-gap when applied in real-world settings. This raises the need of efficient adaptation of policies acting in new environments.

We consider this as a problem of transferring knowledge within a family of similar Markov decision processes. For this purpose we assume that Q-functions are generated by some low-dimensional latent variable. Given such a Q-function, we can find a master policy that can adapt given different values of this latent variable. Our method learns both the generative mapping and an approximate posterior of the latent variables, enabling identification of policies for new tasks by searching only in the latent space, rather than the space of all policies. The low-dimensional space, and master policy found by our method enables policies to quickly adapt to new environments. We demonstrate the method on both a pendulum swing-up task in simulation, and for simulation-to-real transfer on a pushing task.

I. INTRODUCTION

Deep Reinforcement Learning (RL) has been successful in solving a range of complex problems [1]–[5]. Unfortunately, the performance of learned policies may degrade quickly in a slightly different test environment [6]. Also, training is both computationally intense and need considerable amounts of data, making retraining in new environments time consuming. For most real-world settings, such as robotics, difference in training and deployment conditions is common and data collection is costly. This makes fast adaptation and generalization to new environments with few interactions and little computation an important challenge.

To address these issues, it has been suggested to learn a single policy that generalizes well to similar environments [7]–[9], fine-tune policies in new environments [10]–[13], or learn from teacher policies [14]–[17]. Despite recent progress, methods are still limited, e.g., to optimization in large parameter spaces, restrictions in environment differences, types of teacher policies and optimization objectives.

In this work, we propose Variational Policy Embedding (VPE) for learning an adaptable *master policy* for a family of similar Markov Decision Processes (MDPs). Instead of finding one robust policy, the master policy can be easily adapted to new members of the family. Assuming that the

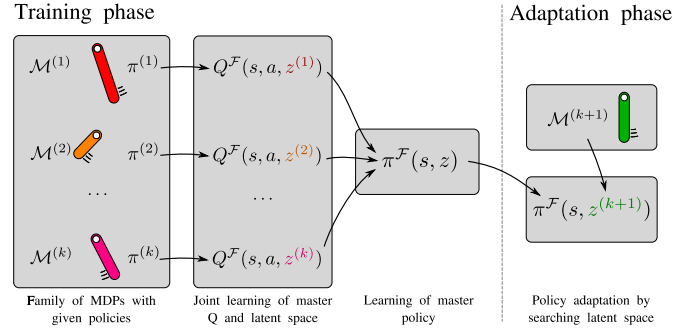


Fig. 1: We are given a set of MDPs \mathcal{M} along with corresponding optimal policies π . All MDPs share the same state and action space, but potentially differ in transition probabilities and reward functions. These differences are assumed to be generated from an unobserved variable z , hence generating a family of MDPs. By learning z and how it generates Q-functions, we are able to transfer knowledge from teacher policies to novel MDPs within the same family.

family is parameterized by some continuous latent variable, we generalize from optimal teacher policies for a set of example members, as illustrated in Fig. 1. For example, a family of swing-up pendulum environments could be parameterized by the mass of the pendulum and the cost to apply a certain torque. Note here that the parameterization can influence both transition probabilities and reward functions.

Instead of identifying the complex relationships between the latent parameter, the family of MDPs, and their optimal policies, we use unsupervised learning to identify a suitable embedding into a latent space, \mathcal{Z} . The latent space can then be used to change the behavior of the master policy. Since different points in the latent space encode optimal policies for the whole family, adaptation for a new member can be carried out in \mathcal{Z} instead of searching the space of all policies. For efficient adaptation it is therefore desirable that \mathcal{Z} is low-dimensional and that its structure is suitable for fast adaption, e.g., by having a locally smooth injection to the space of relevant policies. To achieve this, we use variational Bayesian methods to learn a minimum description length embedding.

Our method is based on the following contributions:

- deriving an evidence lower bound for variational approximation of the latent space,
- enabling lower bound optimization for both stochastic and deterministic teacher policies,
- formulating policy adaption as global optimization in latent space, and

¹Authors are with the Robotics, Perception, and Learning lab, Royal Institute of Technology, Sweden. {isacar, jastork, dani}@kth.se. Correspondence to isacar@kth.se.

- adapting the policy by either Bayesian optimization or stochastic gradient descent.

Our empirical evaluation shows that we can learn the master policy from a set of teacher policies and successfully adapt it to new MDPs with only a few optimization steps. For evaluation, learning the latent space and master policy is carried out in synthetic domains but we also show policy adaptation in a real-world robotic manipulation scenario.

II. RELATED WORK

Transfer learning (TL) deals with knowledge transfer from previous learning, to lessen the need of learning tasks *tabula rasa* [18]. TL have in recent years shown remarkable success in supervised learning for vision [19]–[21]. TL is not only used for supervised learning, but is also a relevant area of research for RL [22]. In the most general case for RL, knowledge is transferred between MDPs with different state and action spaces. We will on the other hand restrict our attention to the case where these are shared over similar MDPs.

Domain randomization attempts to find a single policy that works for all instances of a family [7], [8]. This is feasible in families with small variations in for example friction, but not where good actions are necessarily different between MDPs. We will instead consider finding a policy which can easily be adapted to new MDPs.

In *meta-learning* for RL, the most recent approaches consider learning parameter initializations that only require few gradient steps to change to a new behavior [10], [11]. This has been successfully demonstrated for RL [10], but requires second order gradients. An attempt to simplify the method using only first order gradients was also presented for supervised learning, but was not able to produce successful policies in the RL domain [11]. In addition to using second order gradients for RL, these approaches currently update all parameters, limiting it to gradient descent methods in high-dimensional spaces. Also, training a policy in multiple scenarios simultaneously could be not only challenging, but impossible if environments can not be interacted with simultaneously.

Imitation learning could be used to learn from a set of teacher policies trained in advance [14]–[17]. For imitation learning with supervised learning [14], common loss functions can, however, easily lead to sub-optimal actions. For example, consider approaching a T-junction where demonstrations shows turning either left or right. Regression with a mean squared error loss would result in a policy that drives straight ahead. Instead of learning the mean it was proposed to learn a linear combination of teacher policies [17]. Although avoiding to learn sub-optimal means, the combination vector grows with the number of policies. In our work, the latent space instead only needs as many dimensions as is sufficient to distinguish environments. Another alternative to ill-behaving loss functions is to learn the loss function and a multi-modal policy simultaneously using generative adversarial networks (GANs) [15], [16], [23]. GANs are however notoriously hard to train and convergence

is not guaranteed [24]. We will instead leverage well known methods for supervised learning with temporal difference [25] and variational inference [26].

Previous works have also considered extending Q-functions with a latent space, allowing it to encompass multiple environments and tasks by changing the value of the latent variable [12], [13]. Neitz [12], in contrast to our work, only consider discrete action spaces and does not introduce any principled way to enforce a smooth embedding and minimum description length parameters of the latent variables. Hausman *et al.* [13] on the other hand employs variational inference to allow principled inference of the latent parameters. This is, however, maximizing a trade-off between policy entropy and future rewards instead of solely the discounted sum of future rewards. Also, Hausman *et al.* lower bound the entropy of policies, which applies to stochastic policies. In our work, we present an alternative probabilistic formulation allowing generalization from both stochastic and deterministic policies through optimization of the evidence lower bound.

III. PROBLEM FORMALIZATION AND NOTATION

We consider a *family* of similar MDPs, \mathcal{F} , where each member $\mathcal{M} \in \mathcal{F}$ is defined by a tuple,

$$\mathcal{M} \triangleq (S, A, p_S, p_R, \gamma),$$

with (continuous) state space S and action space A . The constant $\gamma \in \mathbb{R}^+$ denotes the discount factor and a policy is either a mapping $\pi: S \rightarrow A$ or a distribution over actions $\pi: S \times A \rightarrow [0, 1]$. If not stated otherwise, we refer to the deterministic policy. While all members of the family share the same state space and action space, they have different transition probabilities $p_S(s_{t+1}|s_t, a_t)$ or reward distributions

$p_R(r_t|s_t, a_t)$. In all cases, subscript t denotes time and both p_S and p_R are stationary. In our model, the family \mathcal{F} is parameterized by some unobserved variable Z from the domain \mathcal{Z} . For instance, the family of inverted pendulums used in Sec. VI-A is parameterized by the mass of the pendulum and the cost of applying a certain torque.

In the policy adaption scenario we are given or can obtain K optimal policies, $\{\pi^{(i)}\}_{i=1}^K$, for a sample set of family members, $\{\mathcal{M}^{(i)}\}_{i=1}^K \subset \mathcal{F}$. We call these *teacher policies* and *teacher MDPs*. For some new MDP $\mathcal{M}^{(K+1)} \in \mathcal{F}$, our goal is to generalize from the known teacher policies to a new optimal policy $\pi^{(K+1)}$ for $\mathcal{M}^{(K+1)}$ by searching a low-dimensional space and using only few interactions with $\mathcal{M}^{(K+1)}$. To this end, we introduce one single adaptable master policy $\pi^{\mathcal{F}}: S \times \mathcal{Z} \rightarrow A$ that can be adapted to different MDPs of the family. In this formulation, adapting the policy $\pi^{\mathcal{F}}$ to $\mathcal{M}^{(K+1)}$ equals searching \mathcal{Z} for the correct value $z^{(K+1)} \in \mathcal{Z}$.

IV. VARIATIONAL POLICY EMBEDDING

In this section, we explain how we learn the master policy $\pi^{\mathcal{F}}$ for a family of similar MDPs \mathcal{F} , how we identify the structure of the latent space \mathcal{Z} , and how we search \mathcal{Z} to

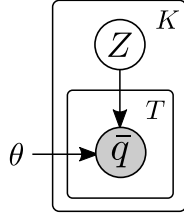


Fig. 2: We consider Q-functions to be generated by a latent variable Z . K is the number of teacher MDPs and T is the number of observed transitions.

adapt to a new and unseen member $\mathcal{M}^{(K+1)}$. Unfortunately, directly modeling $\pi^{\mathcal{F}}$ by interpolating or combining the teacher policies is difficult, not least because multiple optimal policies can exist. Optimal state-action value functions (Q-functions) are on the other hand unique for any MDP [25, p. 50], which makes modeling of one single master Q-function easier. For this reason, we first learn a master Q-function, $Q^{\mathcal{F}}: S \times A \times \mathcal{Z} \rightarrow \mathbb{R}$, for the family \mathcal{F} as a critic for optimizing $\pi^{\mathcal{F}}$ as an actor [27].

We proceed step-by-step, beginning with jointly learning the embedding into \mathcal{Z} and the function $Q^{\mathcal{F}}$ from interactions with the teacher MDPs (Sec. IV-A). In the following step we optimize the master policy $\pi^{\mathcal{F}}$ (Sec. IV-B), and finally, we present two methods of inferring Z for interactions with the test MDP $\mathcal{M}^{(K+1)}$ in order to adapt $\pi^{\mathcal{F}}$ (Sec. IV-C). Implementation details of these steps are given in Sec. V.

A. Latent Space and Master Q-function

In order to learn the latent space embedding to \mathcal{Z} and the master Q-function for the family \mathcal{F} we introduce a generative map from latent space to Q-functions as seen in Fig. 2. For this model, we represent the master Q-function, $Q^{\mathcal{F}}$, as a neural network with parameters θ . Our learning objective is that, for every MDP $\mathcal{M}^{(i)}$, the master Q-function matches the Q-functions that are induced by the known teacher policies $\pi^{(i)}$,

$$Q_{\pi^{(i)}}^{(i)}(s_t, a_t) = \mathbb{E}_{p_S^{(i)}, p_R^{(i)}, \pi^{(i)}} \left[\sum_{h=0}^{\infty} \gamma^h r_{t+h} \mid s_{t+h}, a_{t+h} \right],$$

with the learned parameters θ and latent coordinate $z^{(i)} \in \mathcal{Z}$.

However, in our setting, we only have access to teacher policies $\pi^{(i)}$ and interactions with the teacher MDPs $\mathcal{M}^{(i)}$. The induced Q-functions $Q_{\pi^{(i)}}^{(i)}$ are not observed directly. For this reason, we instead consider state transitions and employ the temporal difference method [25]. An observed value for a transition $(s_t^{(i)}, a_t^{(i)}, s_{t+1}^{(i)}, r_t^{(i)})$ is then given as

$$\bar{q}_t^{(i)} = r_t + \gamma Q^{\mathcal{F}}(s_{t+1}, \pi^{(i)}(s_{t+1}), z^{(i)}), \quad (1)$$

which allows us to use $\bar{q}_t^{(i)}$ as a target for $Q^{\mathcal{F}}(s_t, a_t, z^{(i)})$ in learning. Note that we are not necessarily restricted to deterministic teacher policies. For stochastic policies, we instead use Monte Carlo sampled targets

$$\bar{q}_t^{(i)} = r_t + \gamma Q^{\mathcal{F}}(s_{t+1}, a, z^{(i)}), \quad (2)$$

with sampled actions $a \sim \pi^{(i)}(\cdot \mid s_{t+1})$.

Probabilistic Modeling: We model the problem of jointly learning the embedding to $\mathcal{Z} = \mathbb{R}^d$ and the parameter θ as estimating the latent space posterior distribution. Accordingly, we define $\mathbf{Z} = \{Z^{(i)}\}_{i=1}^K$ as the set of latent variables and $\mathbf{Q} = \{\bar{q}_t^{(i)} : i \in 1, \dots, K, t \in 1, \dots, T\}$ as the set of observations as seen in Fig. 2. The dataset \mathcal{D} consists of transitions $\tau = (s_t^{(i)}, a_t^{(i)}, s_{t+1}^{(i)}, r_t^{(i)}, i)$ for different MDPs.

For the prior distribution we select a multivariate Gaussian with unit variance, $p(\mathbf{Z}) = \prod_{i=1}^K p(Z^{(i)}) = \prod_{i=1}^K \mathcal{N}(\mathbf{0}, \mathbf{I})$, and approximate the posterior distribution $p(\mathbf{Z}|\mathcal{D})$,

$$p(\mathbf{Z}|\mathcal{D}) \approx q(\mathbf{Z}) = \prod_{i=1}^K q_i(Z^{(i)}) = \prod_{i=1}^K \prod_{j=1}^d \mathcal{N}(\mu_j^{(i)}, \sigma_j^2), \quad (3)$$

with one mean vector, $\mu^{(i)} \in \mathbb{R}^d$, for each teacher MDP and a shared vector of variances for each dimension, $\sigma \in \mathbb{R}^d$. The likelihood, $p(\mathcal{D}|\mathbf{Z}, \theta)$, is defined as a product over all transitions in the dataset,

$$p(\mathcal{D}|\mathbf{Z}, \theta) = \prod_{\tau \in \mathcal{D}} p(\bar{q}_t^{(i)} | s_t^{(i)}, a_t^{(i)}, z^{(i)}, \theta). \quad (4)$$

For each transition we model the likelihood with a Gaussian,

$$p(\bar{q}_t^{(i)} | s_t^{(i)}, a_t^{(i)}, z^{(i)}, \theta) = \mathcal{N}(Q^{\mathcal{F}}(s_t, a_t, z^{(i)}), \frac{1}{\lambda^2}), \quad (5)$$

where $\lambda \in \mathbb{R}$ is a small, a-priori chosen constant.

Probabilistic Inference: We infer the parameters of the approximated posterior $\{\mu^{(i)}\}_{i=1}^K$ and σ together with the neural network parameters θ by maximizing the evidence lower bound (ELBO),

$$\mathcal{L}_{\text{ELBO}}(\theta, \mu, \sigma) = \sum_{\tau \in \mathcal{D}} \left(\mathbb{E}_{z \sim q_i} \left[\log p(\bar{q}_t^{(i)} | s_t^{(i)}, a_t^{(i)}, z, \theta) \right] + D_{\text{KL}} \left(q_i(Z^{(i)}) \parallel p(Z^{(i)}) \right) \right) \quad (6)$$

However, by ignoring constants, we can equivalently maximize the following objective:

$$\mathcal{L}(\theta, \mu, \sigma) = \sum_{\substack{\tau \in \mathcal{D} \\ z \sim q_i}} \left(\tau^2 \left(\bar{q}_t^{(i)} - Q^{\mathcal{F}}(s_t^{(i)}, a_t^{(i)}, z) \right)^2 + \sum_{j=1}^d \left(\sigma_d^2 + \mu_d^{(i)2} - \ln \sigma_d^2 \right) \right), \quad (7)$$

where we employ Monte Carlo integration by randomly drawing $z \sim q_i$ in Eq. (7).

Optimization of the objective in Eq. (7) over the parameters μ , σ , and θ serves two purposes. First, it finds parameters of $Q^{\mathcal{F}}$ that are compliant with the latent space embedding to \mathcal{Z} . Second, the optimization is equivalent to minimization of the divergence between the true posterior and the approximate posterior,

$$D_{\text{KL}}(q(\mathbf{Z}) \parallel p(\mathbf{Z}|\mathcal{D})). \quad (8)$$

This means that we are approximating the true posterior in terms of KL-divergence. As a key consequence, the embedding is compressed in terms of information theoretic

description length [28], [29]. In our evaluation in Sec. VII, we accordingly observe that dimensions of the latent space \mathcal{Z} that are not needed to model $Q^{\mathcal{F}}$ fall back to the prior.

B. Learning the Master Policy

After having learned the latent space embedding and the master Q-function for the family \mathcal{F} in Sec. IV-A, we now have to learn the master policy $\pi^{\mathcal{F}}$ that, additionally to states, takes latent coordinates as input. For this, we model the master policy as a neural network with parameters ϕ . We identify the policy parameters ϕ by maximizing the master Q-function similar to actor-critic learning [27],

$$\arg \max_{\phi} \mathbb{E}_{\substack{\tau \in \mathcal{D} \\ z \sim q_i}} \left[Q^{\mathcal{F}} \left(s_t^{(i)}, \pi^{\mathcal{F}}(s_t^{(i)}, z), z \right) \right]. \quad (9)$$

In practice this expectation can be computed with the training dataset \mathcal{D} from in Sec. IV-A.

C. Policy Adaptation in Latent Space

We propose two distinct methods of adapting $\pi^{\mathcal{F}}$ to a given new MDP $\mathcal{M}^{(K+1)}$. Both methods infer the latent coordinates $z^{(K+1)}$ but the methods differ in the optimization objective and the way they interact with the new MDP. Practical details are given in Sec. V.

ELBO Maximization: In this method we search for the correct latent space coordinate by maximizing the bound from Eq. (7) for a new coordinate $\mu^{(K+1)}$. For this, we collect a dataset of transitions in the new MDP. Different from the procedure for learning the latent space embedding and the master Q-function, we keep all parameters but $\mu^{(K+1)}$ fixed.

Bayesian Optimization: In this method, we employ Bayesian optimization (BO) [30] for global search in \mathcal{Z} . To this end, we iteratively interact with the new MDP and collect rollouts with the policy for the current value of $z^{(i)}$. The cost function is defined as rollout performance in the new MDP. To minimize the search space we only consider latent dimensions with large enough mean signal-to-noise ratio (SNR),

$$\text{SNR}_d = \frac{1}{K\sigma_d} \sum_{i=1}^K |\mu_d^{(i)}|. \quad (10)$$

Latent dimensions that are distributed close to the prior, hence not providing information, have signal-to-noise ratio close to zero, and can be disregarded.

V. IMPLEMENTATION DETAILS

In this section, we provide details of how our method described in Sec. IV is implemented for the experiment in Sec. VI. The sections are ordered according to the same structure as in Sec. IV.

A. Latent Space and Master Q-function

For each experiment, we sampled a dataset \mathcal{D} of one million state transitions. Sampling was accomplished by performing ε -greedy rollouts in the teacher MPDs with the corresponding teacher policies. The parameter ε was set to 0.5 but we note that this might not be ideal in general. A small validation set was also collected, and model parameters with the best ELBO on this set was kept for policy fitting.

The master Q-function $Q^{\mathcal{F}}$ was modeled by a 10-layer residual network with 400 ReLU units in each layer and the latent space \mathcal{Z} had 8 dimensions. Target and tracking networks were used for both the parameters θ and the latent space parameters [2].

Training was run for one million gradient descent updates, with each mini-batch containing 32 data points. The KL-divergence term in the loss was linearly increased from zero the first 50 thousand iterations [31]. Target values were generated according to Eq. (1) and were normalized using Pop-Art [32]. Samples from the approximate posterior, state, and action variables were concatenated as a single input to the master Q-function. The state and action space inputs were normalized using Welford's algorithm [33]. The observation noise parameter λ was set implicitly by weighting the likelihood term by 10.0, and the KL-divergence term by 0.001. Adam [34] was used as optimizer.

B. Learning the Master Policy

The same dataset as described in V-A was used to fit the adaptable policy $\pi^{\mathcal{F}}$. The neural network architecture was identical to the one for $Q^{\mathcal{F}}$ with the only difference being the input and output dimensions. Master Q-function and latent space parameters were kept fixed while optimizing Eq. (9). Training was run for 2 million optimization steps, with a batch size of 128. Adam [34] was also used for the actor, with the addition of a weight decay of 0.01. After every 100 gradient updates, an estimate of the mean return was attained by executing rollouts with the policy. The parameters associated with the best return are used for $\pi^{\mathcal{F}}$.

C. Policy Adaption in Latent Space

To find latent space coordinates for a new MDP $\mathcal{M}^{(k+1)}$, we searched over possible assignments of $z^{(k+1)}$ while leaving ϕ unchanged. We evaluated both *ELBO Maximization* and *Bayesian Optimization* (BO). For *ELBO Maximization* we used stochastic gradient descent by repeating the procedure of Sec. V-B, Eq. (7), with a dataset consisting of 16000 state transitions in the new MDP. For evaluation, $z^{(k+1)}$ was deterministic by setting it to the mean $\mu^{(k+1)}$.

BO [30] builds a Gaussian process (GP) posterior of the cost function. As cost function we defined the rollout return given assignments of $z^{(K+1)}$ used the Matérn kernel. As acquisition function, the upper confidence bound of the posterior was used. For the exact details, we refer to the framework of [35]. We used only default values as hyperparameters.

VI. EXPERIMENTS

In the following, we describe two experiments to demonstrate the proposed method. We start with a simpler family of swing-up pendulum MDPs in simulation. We then proceed with a more challenging pushing problem, where we perform policy adaptation on a real-world robotic system.

A. Pendulum Swing-up

We start with the classic control problem of swinging up an inverted pendulum. Although not being a notoriously hard problem, parameterizing both the state transition distribution and the reward distribution is intuitive by changing the mass of the pendulum, and the relative cost of actuating the joint. With this parameterization, we can also make sure that optimal policies for some MDPs can not successfully get the pendulum to upright in other MDPs. This problem also have at least two optimal policies in the state where the pendulum is at rest, pointing down.

We modify the Open AI environment *Pendulum* [36] for our first family of MDPs. Let the pendulum angle from upright be denoted ψ . The action is defined as the acceleration of this angle, $\ddot{\psi}$. We choose two parameters for family generation, one governing the transition dynamics, and one for the reward function. The dynamics is altered by sampling the mass of the pendulum uniformly in $[0.4, 1.2]$. The reward function is altered by a parameter $\kappa \in [0.0, 2.0]$ as follows:

$$r_{\kappa(i)}(\psi, \dot{\psi}, \ddot{\psi}) = -(\psi^2 + 0.1\dot{\psi}^2 + \kappa(i)\ddot{\psi}^2)$$

Before training, 40 teacher MDPs were sampled followed by training of teacher policies for each of the MDPs. Teacher policies were constructed by discretization of the state and action space and performing value iteration with a tabular approximation of the value function [37]. The resulting policies turned out to be sub-optimal, but they all get the pendulum to an upright, stable, position. Policies can however not successfully be used in other MDPs within the family, as expected. In addition to the 40 teacher MDPs/policies, a set of 4 MPDs and policies were added as a test set for policy adaptation. The discount factor γ was set to 0.99. Further details regarding teacher policy training can be found in Appendix A.

B. Non-prehensile Manipulation

To illustrate the method further, we consider a more challenging problem by training the global Q-function and policy in simulation, and then perform evaluation by adapting to a new MDP given by a real-world robotic system. The idea of this experiment is to increase the dimensionality of the problem, and to see if we can accomplish transfer learning from simulation to the real setting. The task is to push a box with varying dynamics to a fixed goal pose. The box that is pushed in the real-world system has a weight placed inside, off-center, serving as the unknown latent variable. By changing the position of the weight, the transition distribution drastically changes, and hence also the behavior of a successful policy. In simulation, the placement

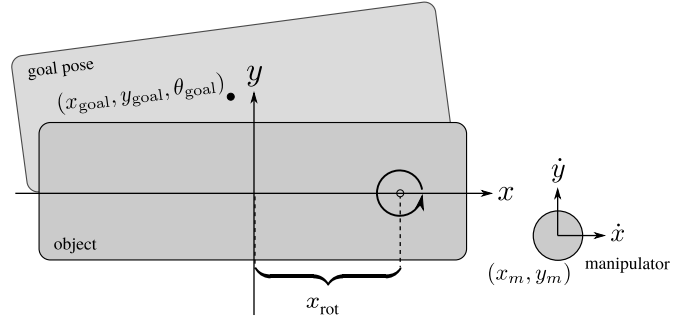


Fig. 3: The second family of MDPs is based on a pushing problem. The aim is to control the velocities of the manipulator such that the object is aligned with the goal pose. The generation of different MDPs is done by offsetting the rotational joint as shown by x_{rot} .

of the weight is accomplished in by offsetting the rotational axis of the box. The problem is illustrated in Fig. 3. The state is denoted by (all in object frame):

$$s = (x_m, y_m, \dot{x}_m, \dot{y}_m, x_{\text{goal}}, y_{\text{goal}}, \theta_{\text{goal}})$$

Here, m refers to the manipulator state.

For the teacher policies, the reward function r was heavily shaped to make training possible (s' denotes successor state):

$$\begin{aligned} r(s, s') &= g(s') - g(s) + h(s') \\ g(s) &= -c_1 \cdot \|(x_{\text{goal}}, y_{\text{goal}}, c_2 \theta'_{\text{goal}})\|_2 \\ &\quad - c_3 \cdot \|(x_m, y_m)\|_2 \\ h(s) &= c_3 \cdot \exp(-c_4 \|(x_{\text{goal}}, y_{\text{goal}}, c_2 \theta_{\text{goal}})\|_2) \end{aligned}$$

The parameters above was set to: $c_1 = 100$, $c_2 = 0.1$, $c_3 = 10$, and $c_4 = 32$. For adaptation on the real robot, this was changed to a simpler reward based solely on the final distance to the goal after one rollout. For simulation, we use the MuJoCo physics simulator [38]. The real-world setup is shown in Fig. 4. The offset of the rotational axis is in simulation sampled uniformly in $[-0.05, 0.05]$, where ± 0.08 corresponds to the outer edges of the box. Also for these MDPs, the discount factor was set to $\gamma = 0.99$.

The training set policies are found by using deterministic policy gradients (DPG)[4]. Further information about learning these policies is described in Appendix B. Implementation details regarding the robotic setup can be found in Appendix C.

C. Policy Adaptation

1) *Pendulum Swing-up*: As an objective function, for a given assignment of $z^{(K+1)}$, we calculated the average return of 4 rollouts with 200 steps each. The seed was set to zero before each call to the objective function. The GP was fitted first after 5 initial samples, then followed by 15 additional optimization steps. In terms of state transitions, this totals $4 \cdot 20 \cdot 200 = 16000$, same as for the gradient descent described above.

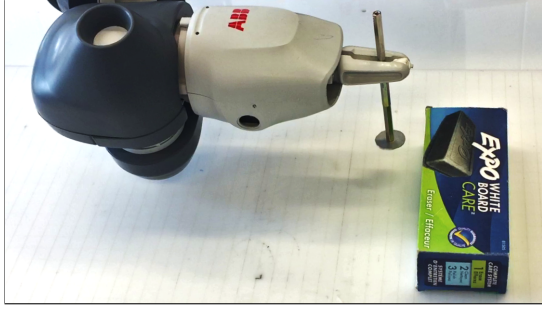


Fig. 4: For pushing, a master policy is first trained in simulation and then adapted on a real-world setup. We use an ABB YuMi robot to push a box using a planar cartesian controller. The box has a weight inside, placed off-center, to make the dynamics challenging.

2) *Non-prehensile Manipulation*: For practical reasons on the real system, the objective function was defined from the final state of one rollout (in object frame):

$$f(x_{\text{goal}}, y_{\text{goal}}, \theta_{\text{goal}}) = -10 \cdot \|(x_{\text{goal}}, y_{\text{goal}}, \frac{\theta_{\text{goal}}}{10})\|_2 \quad (11)$$

This becomes zero when the goal pose is identical to the object pose, otherwise negative. The GP was fitted after 8 rollouts of random $z^{(K+1)}$ assignments, followed by 20 additional rollouts in the optimization procedure.

VII. RESULTS

To demonstrate our method, we will in this section present qualitative and quantitative results regarding both the found embedding, and the performance of the adapted master policy. For the latent space, we want to know whether we see compression of information to a few dimensions, according to signal-to-noise ratio (SNR). We also want to see whether the learned embedding is comparable to the true environment parameters.

A. Pendulum Swing-up

After joint learning of the master Q-function and the embedding, we saw two peaks in the latent space, in terms of SNR. This is shown in Fig. 5, dimensions 0 and 3. To qualitatively assess these dimensions, we plot these dimensions against mass and torque cost κ , shown in Fig. 6. The two parameters are clearly encoded by two orthogonal planes in the latent space. The remaining six dimensions fell back to the prior and was ignored in the adaptation phase.

For policy adaptation, the results can be seen in Table I. Comparison was made between average policies, teacher policies, SGD-trained policies, and BO-trained policies. The average policy value is calculated by repeated draws of z from the prior, performing a rollouts, and averaging the return. A thousand rollouts were performed to calculate the average return and standard error. The suboptimal teacher policies were outperformed by the global policy after adaptation with BO. Stochastic gradient descent produced policies that in some cases were worse than policies drawn randomly

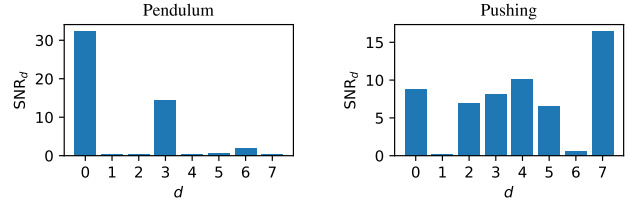


Fig. 5: Mean signal-to-noise ratios (SNR) of found latent space parameters. In both environments, we used the two dimensions with highest SNR for policy adaptation. For the pendulum, dimensions 0 and 3 encode mass and torque cost κ . For the pushing task, dimension 7 corresponds to the rotational offset x_{rot} .

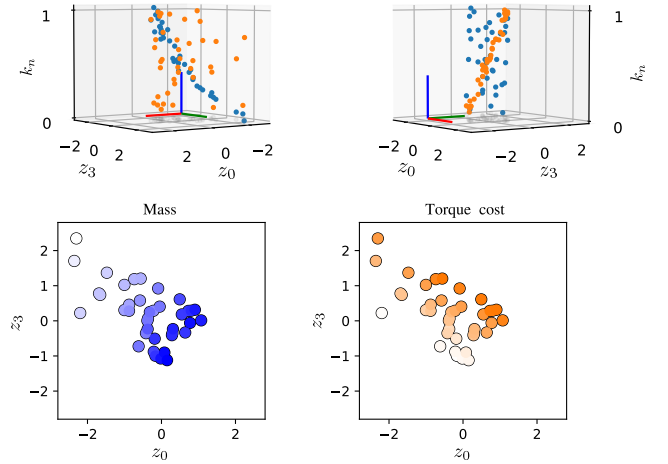


Fig. 6: Found latent space parameters z_0 and z_3 plotted against pendulum mass (blue) and action penalty coefficient (orange). Mass and torque cost are normalized to be in $[0, 1]$ for illustrative purposes. The plots are rotated exactly 90° in the (z_0, z_3) -plane to illustrate that these features are orthogonal, even if z_0 and z_3 are correlated. Bottom plots are showing the same latent space dimensions, but color coded according to the mass and torque cost parameters. Best seen in color.

from the prior, and never outperforming the policies found by BO.

B. Non-prehensile Manipulation

SNR for the learned embedding is shown in Fig. 5. The two dimensions with the highest SNR are plotted against the rotational offset x_{rot} in Fig. 7. Two dimensions equals the prior, and the dimension with the highest SNR clearly encodes the parameter x_{rot} . The other dimensions could not be associated with x_{rot} . Also here, we used the two dimensions with highest SNR for optimization with BO on the real robot. Results of the BO procedure are shown in Fig. 8. The BO procedure, and demonstrations of the final policy can be seen here: <https://youtu.be/OMR7hHNSEKM>.

TABLE I: Comparison of sampled returns in pendulum test environments

#	Average policy	Teacher policy	SGD	20-step BO
1	-134.6 ± 3.0	-97.2 ± 1.6	-105.4 ± 1.6	-90.0 ± 1.5
2	-161.7 ± 4.2	-152.5 ± 2.8	-175.6 ± 2.8	-121.5 ± 2.2
3	-131.0 ± 3.3	-117.0 ± 1.9	-113.6 ± 1.8	-103.0 ± 1.7
3	-188.9 ± 5.0	-181.5 ± 3.0	-274.2 ± 5.1	-136.2 ± 2.6

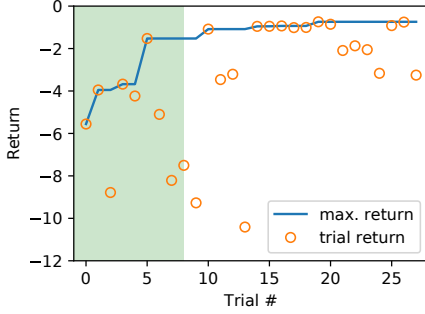


Fig. 8: Bayesian optimization on the real-world pushing task. The green region represent the first random samples of $\mu^{(K+1)}$ before the GP is first fitted. Returns were calculated from the final state in each rollout from Eq. (11).

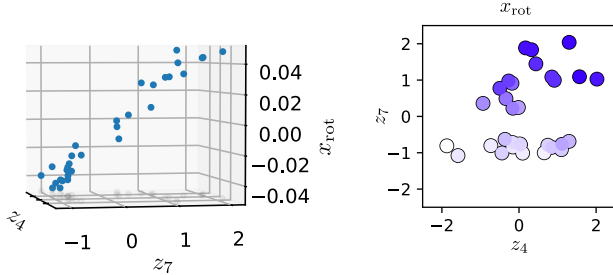


Fig. 7: The parameter x_{rot} encoded in the latent dimension mainly in dimension z_7 .

VIII. DISCUSSION

The results show that the method is able to adjust well to new pendulum and pushing MDPs within few optimization steps using BO. On the real robot, this corresponds to successful policies within five to ten minutes, including both rollouts and GP optimization. This shows that we are indeed able to learn and adapt the master policy to new MDPs.

Regarding the latent space, our results show clear reconstructions of environment parameters in the latent space. These parameters are encoded in the dimensions with the highest SNR, giving us a method of determining importance of latent dimensions and select a low-dimensional space for policy optimization. For the pushing task, dimensions on average had higher SNR than for the pendulum environments even though the true environment parameters were fewer. Note, however, that the latent space encodes only environment differences when policies are optimal. When policies are sub-optimal, the Q-function is no longer unique, and the

latent space possibly encodes both environment parameters and policy differences.

Possible constraints of this method are increased dimensionality and MDP complexity. Since a Q-function contains all expected returns given any action in any state, adding on top of this the ability to interpolate between Q-functions is clearly a challenging task.

IX. CONCLUSION

To enable efficient transfer to new MDPs, we have considered a generative model where latent parameters generate Q-functions. For this, we derived an evidence lower bound for tractable inference of latent space parameters. This allows transfer from stochastic and deterministic teacher policies to novel MDPs. Lower bound optimization compresses the description length of the approximate posterior, which we confirmed in our experiments where latent variables fall closer to the prior. This allows us to select a small subspace suitable for global optimization strategies. We further demonstrated empirically, both in the synthetic domain and for simulator-to-real transfer, that we can adapt the master policy efficiently to new MDPs.

X. FUTURE WORK

In continuation of this research we plan to more closely investigate the consequences of teacher policy sub-optimality, consider on-line adaption scenarios where the MDP changes over time, and explore more complex control tasks.

ACKNOWLEDGMENTS

This work was funded by the Swedish Fund for Strategic Research (SSF) through the project Factories of the Future (FACT). The authors would also like to thank Carlo Rapisarda and Robert Krug for help with the real-robot experiments.

APPENDIX

A. Pendulum value iteration details

The state was tile encoded by discretizing each dimension into both 71 and 93 bins. The action dimension was discretized into 101 bins. The odd number of bins is due to exclusion of the middle value, 0, that happens if you are dividing into an even amount. Value iteration was run for each environment for 4 hours.

B. Pushing teacher policy details

Deterministic policy gradients (DPG) were used to construct the teacher policies [4]. Parameter space noise for exploration was used, and the architecture of the actor and critic proposed along with that method was used [39]. Online normalization of states and actions was done using Welford’s algorithm [33]. Target values were normalized using Pop-Art [32].

C. Robotic setup

An ABB YuMi robot was used for the pushing experiments using a planar cartesian controller. The object was tracked using SimTrack [40]. Velocities were set slow enough for the box to behave quasistatically.

REFERENCES

- [1] D. Silver, A. Huang, C. J. Maddison, A. Guez, L. Sifre, G. Van Den Driessche, J. Schrittwieser, I. Antonoglou, V. Panneershelvam, M. Lanctot, *et al.*, “Mastering the game of go with deep neural networks and tree search,” *Nature*, vol. 529, no. 7587, p. 484, 2016.
- [2] V. Mnih, K. Kavukcuoglu, D. Silver, A. A. Rusu, J. Veness, M. G. Bellemare, A. Graves, M. Riedmiller, A. K. Fidjeland, G. Ostrovski, *et al.*, “Human-level control through deep reinforcement learning,” *Nature*, vol. 518, no. 7540, p. 529, 2015.
- [3] S. Levine, C. Finn, T. Darrell, and P. Abbeel, “End-to-end training of deep visuomotor policies,” *The Journal of Machine Learning Research*, vol. 17, no. 1, pp. 1334–1373, 2016.
- [4] T. P. Lillicrap, J. J. Hunt, A. Pritzel, N. Heess, T. Erez, Y. Tassa, D. Silver, and D. Wierstra, “Continuous control with deep reinforcement learning,” *arXiv preprint arXiv:1509.02971*, 2015.
- [5] K. Arulkumaran, M. P. Deisenroth, M. Brundage, and A. A. Bharath, “Deep reinforcement learning: A brief survey,” *IEEE Signal Processing Magazine*, vol. 34, no. 6, pp. 26–38, 2017.
- [6] K. Bousmalis, A. Irpan, P. Wohlhart, Y. Bai, M. Kelcey, M. Kalakrishnan, L. Downs, J. Ibarz, P. Pastor, K. Konolige, *et al.*, “Using simulation and domain adaptation to improve efficiency of deep robotic grasping,” *arXiv preprint arXiv:1709.07857*, 2017.
- [7] J. Tobin, R. Fong, A. Ray, J. Schneider, W. Zaremba, and P. Abbeel, “Domain randomization for transferring deep neural networks from simulation to the real world,” in *Intelligent Robots and Systems (IROS), 2017 IEEE/RSJ International Conference on*. IEEE, 2017, pp. 23–30.
- [8] R. Antonova, S. Cruciani, C. Smith, and D. Kragic, “Reinforcement learning for pivoting task,” *arXiv preprint arXiv:1703.00472*, 2017.
- [9] N. Tajbakhsh, J. Y. Shin, S. R. Gurudu, R. T. Hurst, C. B. Kendall, M. B. Gotway, and J. Liang, “Convolutional neural networks for medical image analysis: Full training or fine tuning?” *IEEE transactions on medical imaging*, vol. 35, no. 5, pp. 1299–1312, 2016.
- [10] C. Finn, P. Abbeel, and S. Levine, “Model-agnostic meta-learning for fast adaptation of deep networks,” *arXiv preprint arXiv:1703.03400*, 2017.
- [11] A. Nichol and J. Schulman, “Reptile: a scalable metalearning algorithm,” *arXiv preprint arXiv:1803.02999*, 2018.
- [12] A. Neitz, “Deep q-embedding for transfer reinforcement learning,” *Master Thesis*, 2017.
- [13] K. Hausman, J. T. Springenberg, Z. Wang, N. Heess, and M. Riedmiller, “Learning an embedding space for transferable robot skills,” in *International Conference on Learning Representations*, 2018. [Online]. Available: <https://openreview.net/forum?id=rk07ZXZRb>
- [14] Y. Duan, M. Andrychowicz, B. Stadie, O. J. Ho, J. Schneider, I. Sutskever, P. Abbeel, and W. Zaremba, “One-shot imitation learning,” in *Advances in neural information processing systems*, 2017, pp. 1087–1098.
- [15] K. Hausman, Y. Chebotar, S. Schaal, G. Sukhatme, and J. J. Lim, “Multi-modal imitation learning from unstructured demonstrations using generative adversarial nets,” in *Advances in Neural Information Processing Systems*, 2017, pp. 1235–1245.
- [16] J. Ho and S. Ermon, “Generative adversarial imitation learning,” in *Advances in Neural Information Processing Systems* 29, D. D. Lee, M. Sugiyama, U. V. Luxburg, I. Guyon, and R. Garnett, Eds. Curran Associates, Inc., 2016, pp. 4565–4573. [Online]. Available: <http://papers.nips.cc/paper/6391-generative-adversarial-imitation-learning.pdf>
- [17] C. Zhang, Y. Yu, and Z.-H. Zhou, “Learning environmental calibration actions for policy self-evolution,” in *IJCAI*, 2018, pp. 3061–3067.
- [18] S. J. Pan, Q. Yang, *et al.*, “A survey on transfer learning,” *IEEE Transactions on knowledge and data engineering*, vol. 22, no. 10, pp. 1345–1359, 2010.
- [19] M. Oquab, L. Bottou, I. Laptev, and J. Sivic, “Learning and transferring mid-level image representations using convolutional neural networks,” in *Proceedings of the IEEE conference on computer vision and pattern recognition*, 2014, pp. 1717–1724.
- [20] J. Long, E. Shelhamer, and T. Darrell, “Fully convolutional networks for semantic segmentation,” in *Proceedings of the IEEE conference on computer vision and pattern recognition*, 2015, pp. 3431–3440.
- [21] A. Karpathy, G. Toderici, S. Shetty, T. Leung, R. Sukthankar, and L. Fei-Fei, “Large-scale video classification with convolutional neural networks,” in *Proceedings of the IEEE conference on Computer Vision and Pattern Recognition*, 2014, pp. 1725–1732.
- [22] M. E. Taylor and P. Stone, “Transfer learning for reinforcement learning domains: A survey,” *Journal of Machine Learning Research*, vol. 10, no. Jul, pp. 1633–1685, 2009.
- [23] I. Goodfellow, J. Pouget-Abadie, M. Mirza, B. Xu, D. Warde-Farley, S. Ozair, A. Courville, and Y. Bengio, “Generative adversarial nets,” in *Advances in neural information processing systems*, 2014, pp. 2672–2680.
- [24] L. Mescheder, S. Nowozin, and A. Geiger, “The numerics of gans,” in *Advances in Neural Information Processing Systems*, 2017, pp. 1825–1835.
- [25] R. S. Sutton, A. G. Barto, *et al.*, *Reinforcement learning: An introduction*. Second edition, in progress. MIT press, 2017.
- [26] M. I. Jordan, Z. Ghahramani, T. S. Jaakkola, and L. K. Saul, “An introduction to variational methods for graphical models,” *Machine learning*, vol. 37, no. 2, pp. 183–233, 1999.
- [27] I. Grondman, L. Busoniu, G. A. Lopes, and R. Babuska, “A survey of actor-critic reinforcement learning: Standard and natural policy gradients,” *IEEE Transactions on Systems, Man, and Cybernetics, Part C (Applications and Reviews)*, vol. 42, no. 6, pp. 1291–1307, 2012.
- [28] G. E. Hinton and D. Van Camp, “Keeping the neural networks simple by minimizing the description length of the weights,” in *Proceedings of the sixth annual conference on Computational learning theory*. ACM, 1993, pp. 5–13.
- [29] A. Graves, “Practical variational inference for neural networks,” in *Advances in neural information processing systems*, 2011, pp. 2348–2356.
- [30] J. Moćkus, “On bayesian methods for seeking the extremum,” in *Optimization Techniques IFIP Technical Conference*. Springer, 1975, pp. 400–404.
- [31] C. K. Sønderby, T. Raiko, L. Maaløe, S. K. Sønderby, and O. Winther, “How to train deep variational autoencoders and probabilistic ladder networks,” *arXiv preprint arXiv:1602.02282*, 2016.
- [32] H. P. van Hasselt, A. Guez, M. Hessel, V. Mnih, and D. Silver, “Learning values across many orders of magnitude,” in *Advances in Neural Information Processing Systems*, 2016, pp. 4287–4295.
- [33] B. Welford, “Note on a method for calculating corrected sums of squares and products,” *Technometrics*, vol. 4, no. 3, pp. 419–420, 1962.
- [34] D. P. Kingma and J. Ba, “Adam: A method for stochastic optimization,” *arXiv preprint arXiv:1412.6980*, 2014.
- [35] F. Nogueira, “Bayesian optimization,” <https://github.com/fmfn/BayesianOptimization>, 2018.
- [36] G. Brockman, V. Cheung, L. Pettersson, J. Schneider, J. Schulman, J. Tang, and W. Zaremba, “Openai gym,” 2016.
- [37] R. Bellman, “A markovian decision process,” *Journal of Mathematics and Mechanics*, pp. 679–684, 1957.
- [38] E. Todorov, T. Erez, and Y. Tassa, “Mujoco: A physics engine for model-based control,” in *Intelligent Robots and Systems (IROS), 2012 IEEE/RSJ International Conference on*. IEEE, 2012, pp. 5026–5033.
- [39] M. Plappert, R. Houthoofd, P. Dhariwal, S. Sidor, R. Y. Chen, X. Chen, T. Asfour, P. Abbeel, and M. Andrychowicz, “Parameter space noise for exploration,” in *International Conference on Learning Representations*, 2018. [Online]. Available: <https://openreview.net/forum?id=ByBA12eAZ>
- [40] K. Pauwels and D. Kragic, “Simtrack: A simulation-based framework for scalable real-time object pose detection and tracking,” in *Intelligent Robots and Systems (IROS), 2015 IEEE/RSJ International Conference on*. IEEE, 2015, pp. 1300–1307.